Journal Pre-proof

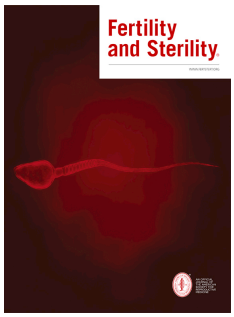

Predicting risk of endometrial failure: a biomarker signature that identifies a novel disruption independent of endometrial timing in patients undergoing hormonal replacement cycles

Patricia Diaz-Gimeno, Ph.D., Patricia Sebastian-Leon, Ph.D., Katharina Spath, Ph.D., Diana Marti-Garcia, M.Sc., Josefa Maria Sanchez-Reyes, Ph.D., Maria del Carmen Vidal, Ph.D., Almudena Devesa-Peiro, Ph.D., Immaculada Sanchez-Ribas, Ph.D., Asunta Martinez-Martinez, M.Sc., Nuria Pellicer, M.D., Ph.D., Dagan Wells, Ph.D., Antonio Pellicer, M.D., Ph.D.

PII: S0015-0282(24)00190-0

DOI: https://doi.org/10.1016/j.fertnstert.2024.03.015

Reference: FNS 34706

To appear in: *Fertility and Sterility*

Received Date: 17 May 2023

Revised Date: 14 March 2024

Accepted Date: 18 March 2024

Please cite this article as: Diaz-Gimeno P, Sebastian-Leon P, Spath K, Marti-Garcia D, Sanchez-Reyes JM, Vidal MdC, Devesa-Peiro A, Sanchez-Ribas I, Martinez-Martinez A, Pellicer N, Wells D, Pellicer A, Predicting risk of endometrial failure: a biomarker signature that identifies a novel disruption independent of endometrial timing in patients undergoing hormonal replacement cycles, *Fertility and Sterility* (2024), doi: https://doi.org/10.1016/j.fertnstert.2024.03.015.

Running title: Endometrial Failure Risk (EFR) signature

Predicting risk of endometrial failure: a biomarker signature that identifies a novel disruption independent of endometrial timing in patients undergoing hormonal replacement cycles

Patricia Diaz-Gimeno, Ph.D.,[a*†]

Patricia Sebastian-Leon, Ph.D.[a †]

Katharina Spath, Ph.D.[b]

Diana Marti-Garcia, M.Sc.[a]

Josefa Maria Sanchez-Reyes, Ph.D.[a,c]

Maria del Carmen Vidal, Ph.D.[a,d]

Almudena Devesa-Peiro, Ph.D.[a,c]

Immaculada Sanchez-Ribas, Ph.D.[a,e]

Asunta Martinez-Martinez, M.Sc.[a]

Nuria Pellicer, M.D., Ph.D. [a,d]

Dagan Wells, Ph.D.[b,f]

Antonio Pellicer, M.D., Ph.D.[a,b,c,g]

[a] IVIRMA Global Research Alliance, IVI Foundation, Instituto de Investigación Sanitaria La Fe (IIS La Fe), Av. Fernando Abril Martorell 106, Torre A, Planta 1ª, 46026, Valencia, Spain

[b] JUNO Genetics, Winchester House, Heatley Rd. Oxford Science Park, Oxford, OX4 4GE, United Kingdom

[c] Department of Pediatrics, Obstetrics and Gynecology, University of Valencia, Av.

Blasco Ibáñez 15, 46010, Valencia, Spain

[d] IVI RMA Valencia, Plaza de la policía local nº 3, 46015 Valencia, Spain

[e] IVI RMA Barcelona, Ronda del General Mitre, 14, 08017 Barcelona, Spain

[f] Nuffield Dept. of Women's & Reproductive Health, University of Oxford, Level 3, Women's Centre John Radcliffe Hospital, Oxford, OX3 9DU, United Kingdom

[g] IVI RMA Rome, Largo Il de brando Pizzetti, 1 - Piano Rialzato, 00197, Roma, Italy

[†] P.D.-G and P.S.-L. contributed equally to this work and should be regarded as joint First Authors.

***Corresponding author:** Patricia Diaz-Gimeno

Tel: +34 96 390 33 05

email: patricia.diaz@ivirma.com / patricia_diaz@iislafe.es

IVI Foundation, Biopolo La Fe – Instituto de Investigacion Sanitaria La Fe, Av. Fernando Abril Martorell 106, Torre A, Planta 1ª, 46026, Valencia, Spain.

Article type: Reproductive Biology

Funding statement: This research was funded by the IVI Foundation (1810-FIVI-066-PD and 1810-FIVI-048-PD). P.D.-G. was supported by the Instituto de Salud Carlos III (ISCIII; Spanish Ministry of Science and Innovation) through the Miguel Servet program (CP20/00118) co-founded by the European Union, and a visiting scientist fellowship funded by the Generalitat Valenciana at Oxford University (BEST/2019/121). P.S.-L. was funded by ISCIII through the Sara Borrell program (CD21/0132) co-founded by the European Union. Financial support to researchers

was also provided by the Spanish Ministry of Science, Innovation and Universities (APOTIP/2021/048 [A.D.-P], CIAPOT/2021/13 [A.M.-M], ACIF/2018/072 [J.M.S.-R] and FPU/19/03247 [D.M.-G.]).

Disclosure statement: The authors have no conflicts of interest.

Attestation statements:

Data regarding any of the subjects in the study has not been previously published unless specified.

Data will be made available to the editors of the journal for review of query upon request.

Word count: 350 words for abstract and 3993 words for text (from introduction to discussion)

Trial registration: N/A

Capsule: A biomarker signature for a novel endometrial disruption independent of endometrial luteal phase timing accurately identifies IVF patients with poor endometrial prognosis and a >3-fold increased risk of endometrial failure.

ABSTRACT

Objective: To propose a new gene expression signature that identifies endometrial disruptions independent of endometrial luteal phase timing and predicts if patients are at risk of endometrial failure.

Design: Multicentric, prospective study.

Setting: Reproductive medicine research department in a public hospital affiliated with private fertility clinics and a reproductive genetics laboratory.

Patient(s): Caucasian women (n=281; 39.4±4.8 years old with a BMI of 22.9±3.5 kg/m^2) undergoing hormone replacement therapy between July 2018 and July 2021. Endometrial samples from 217 patients met RNA quality criteria for signature discovery and analysis.

Intervention(s): Endometrial biopsies collected in the mid-secretory phase.

Main Outcome Measure(s): Endometrial luteal phase timing-corrected expression of 404 genes and reproductive outcomes of the first single embryo transfer (SET) following biopsy collection to identify prognostic biomarkers of endometrial failure.

Result(s): Removal of endometrial timing variation from gene expression data allowed patients to be stratified into poor (n=137) or good (n=49) endometrial prognosis groups based on their clinical and transcriptomic profiles. Significant differences were found between endometrial prognosis groups in terms of reproductive rates: pregnancy (44.6% vs. 79.6%, p-value=3.8E-5), live birth (25.6% vs. 77.6%, p-value=5E-10), clinical miscarriage (22.2% vs. 2.6%, p-value=0.0066), and biochemical miscarriage (20.4% vs. 0%, p-value=0.0023). The relative risk of endometrial failure for patients predicted as a poor endometrial prognosis was 3.3-times higher than those with a good prognosis. The differences in gene expression between both profiles were proposed as a biomarker, coined the Endometrial Failure Risk (EFR) signature. Poor

prognosis profiles were characterized by 59 up-regulated and 63 down-regulated genes mainly involved in regulation (17.0%), metabolism (8.4%), immune response and inflammation (7.8%). This EFR signature had a median accuracy of 0.92 (min=0.88, max=0.94), median sensitivity of 0.96 (min=0.91, max=0.98), and median specificity of 0.84 (min=0.77, max=0.88), positioning itself as a promising biomarker for endometrial evaluation.

Conclusion(s): The EFR signature revealed a novel endometrial disruption, independent of endometrial luteal phase timing, present in 73.7% of patients. This EFR signature stratified patients into two significantly distinct and clinically relevant prognosis profiles providing opportunities for personalized therapy. Nevertheless, further validations are needed prior to implementing this gene signature as an artificial intelligence (AI)-based tool to reduce the risk of patients experiencing endometrial failure.

Key words *(10/10)***:** endometrial prognosis, artificial intelligence, machine learning, endometrial timing, precision medicine, patient stratification, endometrial-factor infertility, gene expression signature, endometrial transcriptomics, window of implantation displacement.

INTRODUCTION

A key factor for reproductive success in assisted reproduction treatments (ARTs) is the status of the maternal endometrium during embryo implantation and fetal development. The endometrial cycle is reflected by the cyclic structural and functional changes of the endometrium across the menstrual cycle, and particularly during the mid-secretory phase, to prepare for the “window of implantation” (WOI) (1–5). Following successful embryo implantation, the decidua (specialized layer of the endometrium) actively encapsulates the trophectoderm to support placentation and provide adequate vascularization for optimal fetal growth (6). Thus, approaches that predict and prevent endometrial-factor infertility could substantially improve ART outcomes by supporting the establishment and maintenance of pregnancy (7,8).

There is a lack of consensus in the minimum number of implantation failures with good-quality embryos derived from ovum donation or with confirmed euploid karyotypes required to diagnose recurrent implantation failure (RIF) (9,10). The disparities in clinical classification and heterogeneous etiology of RIF confounds its diagnosis and leaves the exact prevalence unclear (9–14). As clinical symptoms cannot be prevented and do not provide sufficient criteria to stratify patients, patients might be misclassified and receive inefficient treatment. Indeed, most studies using clinical criteria for RIF identified no or few differentially expressed genes between samples of affected patients (15,16), reflecting the molecular heterogeneity of RIF.

To overcome these healthcare challenges, high-throughput molecular technologies are combined with artificial intelligence (AI) algorithms to provide a deeper

understanding of infertility-related pathogenesis (7,17–21). These molecular insights are then applied in genomics-driven precision medicine approaches to characterize complex diseases, and ultimately, improve patient diagnosis and prognosis (22). Employing genomics in reproductive medicine has the potential to go beyond treating the clinical manifestations of disease progression (23), by leveraging the patients' heterogeneous molecular profiles for precise stratification and revealing new targets for preventive measures (24–26).

In this regard, current diagnostic tools for endometrial-factor infertility use transcriptomics to date the endometrial biopsy in the mid-secretory phase, exceeding the accuracy and objectivity of traditional endometrial progression staging by Noyes' histological criteria (1,7,17,19,20). However, the clinical utility of synchronizing the endometrium by adjusting the timing of progesterone administration based on the patient's transcriptomic endometrial dating profile remains controversial (27–34). Independent randomized clinical trials found no improvement in reproductive outcomes (34), indicating the inefficacy of this clinical intervention and highlighting the need for alternative treatments and/or a refined target patient population that benefits from this strategy.

Combining these precision medicine approaches with transcriptomics and AI algorithms; our group recently proposed a novel molecular taxonomy of RIF and a new clinical algorithm for endometrial-factor infertility that considered two molecular causes of implantation failure: a WOI displacement that indicates a dysregulated endometrial timing; and a WOI disruption that indicates an endometrial alteration independent of endometrial timing (18). Transcriptomic analysis revealed these two WOI phenotypes

were presented exclusively or simultaneously and patients with RIF had significantly more WOI disruptions but similar frequency of WOI displacements, compared to controls (18). These findings suggested WOI disruptions had stronger associations to implantation failure than WOI displacements and shifted the paradigm for the study and treatment of endometrial-factor infertility (18). In addition, this work by Sebastian-Leon *et al.* highlighted the importance of removing the transcriptomic variation due to cyclical endometrial tissue changes (i.e., the effect of endometrial timing) that, if not corrected, could mask the significant disruptions in endometrial gene expression (15,16). However, given this hypothesis-driven research was conducted retrospectively and *in silico* with publicly available data, the reproductive outcomes of the cycle following the biopsy collection were not available (15). This clinical follow-up is required to discover biomarkers for WOI disruption in patients with a higher risk of endometrial failure.

Based on these genomics-driven precision medicine strategies, this proof-of-concept study aimed to discover a biomarker panel that could identify endometrial disruption, independent of endometrial timing, to predict, and ultimately prevent, poor reproductive outcomes in in vitro fertilization (IVF) patients.

MATERIAL AND METHODS

Ethics statement

This study was approved by the Ethics Committee of the Instituto Valenciano de Infertilidad, Valencia, Spain (1810-FIVI-066-PD/1810-FIVI-048-PD). Written informed consent was obtained from all recruited patients (n=281).

Participants, collection of endometrial biopsies and reproductive outcomes

This prospective, multicentric study was conducted between July 2018 and July 2021 at five private fertility clinics in Spain. Participants (n=281) were scheduled for endometrial evaluation due to medical indications or ≥2 implantation failures of idiopathic origin. All patients met the following inclusion criteria: 18-50 years old, with a body mass index (BMI) of 19-30 kg/m^2, undergoing hormone replacement therapy for SET, presenting an endometrial thickness >6.5 mm with trilaminar structure in proliferative phase before progesterone administration, and serum levels of estradiol (E2) >100 pg/mL and progesterone (P4) <1 ng/mL on the tenth day of estrogen treatment (17). Endometrial biopsies were collected following an average of 114.5 ± 7.2 h of progesterone (duration ranged from 82 to 172 h), and processed as we previously described (17).

Baseline patient characteristics including age, BMI, the number of IVF attempts, the quality of the embryo transferred (defined in the Supplemental Methods), and reproductive outcomes (i.e., pregnancy, live birth, biochemical and clinical miscarriage) for each attempt, were obtained from internal medical records. Information about IVF attempts in other fertility clinics was included if recorded (only in 47.7% of patients).

Study design

First, a custom RNA-seq gene panel [the Endometrial Failure Risk (EFR) panel] comprising 404 biomarkers of endometrial luteal phase timing and/or potential disruption was designed and employed to determine the risk of endometrial failure among 217 IVF patients (Supplemental Figure 1.1). The endometrial timing-corrected

expression of the EFR panel was used to study the differential expression associated to endometrial disruption together with clinical characteristics of IVF patients to stratify the population as having poor or good endometrial prognoses, according to a semi-supervised learning process (Supplemental Figure 1.2). The distinct transcriptomic patterns of each prognosis group were associated to the differences in reproductive outcomes of SET following biopsy collection, and the differentially expressed gene signature was proposed as biomarker of endometrial disruption (Supplemental Figure 1.3). Finally, the gene expression signature was used to supervise machine learning algorithms to evaluate the biomarker capacity of this signature to distinguish endometrial competence. The predictive performance of the models was assessed through the accuracy, sensibility, and specificity over 100 iterations of five-fold stratified cross-validation (Supplemental Figure 1.4).

Constructing the Endometrial Failure Risk (EFR) gene panel

Supplemental Figure 2 illustrates the workflow for the EFR panel gene selection. A whole-transcriptome endometrial dataset (GSE58144, n=115) retrieved from Gene Expression Omnibus (GEO) (35) was processed to correct the endometrial progression effect, using linear models in limma (version 3.46.0) (36), and unmask genes related to endometrial disruption (16). These genes were ranked according to an informativity score (CorrelationAttributeEval) in Weka (version 3.8.2, 2017-12-22) (37) to evaluate their worth by measuring their correlation with endometrial pathology. Gene sets with increasing gene signature size were developed by adding the most informative genes in a stepwise manner, and their predictive performance was analyzed using Support Vector Machine (SVM) (38) and Random Forest (RF) (39) algorithms. After calculating predictive performance with a stratified 5-fold cross-

validation (default parameters; 80:20; 100 iterations) using the Weka R package (40), optimal signature size was determined for each algorithm, as the one with the fewest genes and highest accuracy. Finally, genes we previously prioritized for transcriptomic endometrial dating (17) were also included in the EFR panel to be able to remove the endometrial luteal phase timing variation.

Endometrial biopsy processing, sequencing and transcriptomic preprocessing

Total RNA was extracted, and only samples that met our quality criteria were sequenced using the TruSeq Targeted RNA Illumina protocol and our custom EFR panel, in the Illumina NextSeq 550 platform with a paired-end design of 150 cycles and 4M reads/sample, as previously described (17). Raw transcriptomic data was processed and normalized using limma, to filter low-quality raw counts (Q<30) and low-read samples (<2M) (17). Possible batch effects were detected using principal components analysis (PCA) and corrected with linear models in limma. Finally, endometrial luteal phase timing effects were detected using our TED model (17) (see Supplemental Methods) and removed using limma.

EFR biomarker signature identification

A preliminary classification of patients was based on the patients' history of reproductive outcomes and transcriptomic patterns corrected for endometrial luteal phase timing. This approach eliminated the gene expression variation related to the cyclic tissue changes that mask endometrial disruption (16,18), and was used prior to applying semi-supervised machine learning based on self-labelled techniques (see Supplemental Methods) (41).

Once, the genomic-driven disease taxonomy was established, the differentially expressed genes obtained between the final good and poor prognosis groups were proposed as the EFR biomarker signature. The limma R package was used to identify the statistically significant differentially expressed genes [false discovery rate (FDR)-adjusted p-value<0.05].

Functional characterization of the EFR signature

The biomarker signature genes were annotated for functional interpretation databases by consulting Kyoto Encyclopaedia of Genes and Genomes (KEGG) human pathways (42) (release 99.0, 2021-08-01) and Gene Ontology (GO; version 2021-07-02; employing only experimental annotations) (43). Functional terms were manually summarized into categories according to their description in the database and presented as a bar plot using ggplot2 (44).

EFR signature capability as biomarker of endometrial disruption

To estimate the prediction capability of the EFR signature to distinguish poor and good endometrial prognosis profiles, we implemented predictive models based on SVM algorithm. Using a stratified 5-fold cross-validation process (repeated 100 times), the accuracy, sensitivity, and specificity were estimated. The range of values obtained across the 100 iterations were presented as a boxplot using ggplot2.

Statistical analysis

Rates for reproductive outcomes [i.e., pregnancy rate (PR), cumulative pregnancy rate (CPR), live birth rate (LBR), biochemical miscarriage rate (BMR), and clinical miscarriage rate (CMR)] were calculated as defined in the Supplemental Methods.

Descriptive statistics were used for transcriptomic and clinical characteristics of patients to compare prognosis or WOI displacement groups. Continuous variables were presented as an overall mean ± standard deviation while discrete variables were presented as counts and percentages. Groups were compared using Wilcoxon rank-sum test for continuous variables and Fisher's exact test for discrete variables. All statistical analyses were conducted in R. All graphical results were generated with ggplot2.

Gene expression validation by RT-qPCR

Quantitative real-time polymerase chain reaction (RT-qPCR) was performed to validate the expression of the top four differentially expressed genes between patients with poor (n=10) and good (n=10) endometrial prognoses. RNA (200-220 ng) was reverse transcribed into cDNA using the PrimeScript Reagent Kit (Perfect Real Time, Takara, Japan) on a Thermocycler T3000 (Biometra, Ireland). RT-qPCR was performed on a StepOnePlus Real-Time PCR System (Applied Biosystems, USA) using Power-Up SYBR Green (Thermo Fisher Scientific, USA) and standard conditions. Supplemental Table 1 lists the specific primers (Invitrogen, Thermo Fisher Scientific) used. Universal human RNA (Agilent, Spain) and water were respectively included as positive and negative controls. Each sample was analyzed in duplicate and relative gene expression (normalized to beta actin) was calculated using the ΔΔCt method (50).

RESULTS

Preliminary sequencing with the 404-gene EFR panel

The EFR panel evaluated 404 genes: 139 that predict endometrial disruption and 310

that serve as biomarkers of endometrial dating or timing. Notably, 45 genes overlapped in these two endometrial factors.

Of the 281 endometrial samples collected, we excluded 56 samples for having low-quality or insufficient RNA; six samples containing a low number of sequencing reads (Supplemental Figure 3A); and two samples that had low gene expression after normalization (Supplemental Figure 3B). Thus, 217 patients were considered in the downstream analysis. After correcting batch effects from sequencing runs (Supplemental Figure 3C) and removing the transcriptomic variation due to endometrial cyclic changes (endometrial luteal phase timing; Supplemental Figure 3D), there were no other confounding technical or clinical factors (Supplemental Figure 4).

A genomic-driven endometrial taxonomy for patient stratification based on a novel endometrial disruption independent of endometrial timing

Fourty-four patients were initially categorized as acute RIF (aRIF) based on the inability to carry a pregnancy to term following 3 to 9 SETs. Alternatively, 40 patients were categorized as acute Fertile (aFertile) because they reached full-term pregnancy at the first SET after biopsy. Notably, following this clinical acute criteria, 133 (61.3%) patients remained unclassified for having insufficient attempts (Supplemental Figure 5A) and no transcriptomic differences were found between the aRIF and aFertile groups (the lowest FDR was 0.3027). Incorporation of transcriptomic data with this initial acute clinical classification allowed us to stratify patients with poor (n=137, 63.1%) or good (n=49, 22.6%) endometrial prognoses; leaving only 31 samples

(14.3%) unclassified due to the lack of recognition by the algorithms (Supplemental Figure 5B).

EFR biomarker signature identification and functional characterization

122 genes were identified as significantly different (30.2% of all panel genes, FDR<0.05) between patients with good and poor endometrial prognoses, including 63 down-regulated and 59 up-regulated in patients with poor endometrial prognosis (Table 1 and Figure 1A), and proposed as the EFR biomarker signature. Transcriptomically, endometrial biopsies clustered by prognosis (Figure 1B) and the signature genes had functions that were mainly related to regulation (17%); metabolism (8.4%), the immune system and inflammation (7.8%); protein processes (7.3%), signalling (6.9%), transport (6.1%), the cell cycle, proliferation and differentiation (5.3%) (Figure 1C and Supplemental Table 2). The poor prognosis profile was distinguished by a down-regulation of 27/39 (69.2%) functional groups. We highlight the functions with higher proportions of down-regulated genes as steroidogenesis and steroid signalling (77.8%), hormone-related (80.0%), the nervous system (81.3%), gametogenesis and reproduction (85.7%), oxidative stress and response to O_2 (88.9%), as well as cell action potential and polarization (100%) (Figure 1D). Few functional groups, including cell migration, extracellular matrix and glucose homeostasis contained a larger proportion of up-regulated genes (60.9%, 62.5% and 62.5% up-regulated genes, respectively; Figure 1D).

Differences in clinical reproductive outcomes authenticated the EFR signature's clinical relevance

There were no significant differences in the age or BMI of patients predicted to have good/poor endometrial prognosis (all p>0.05). Women predicted to have poor endometrial prognosis previously underwent significantly more SETs than those with good endometrial prognosis (2.8 vs. 1.6; p<0.0001), however, there were no significant differences in embryo quality (p=0.4679) between groups (Supplemental Table 3). The lack of differences in the proportion of out-of-phase endometria (57% in poor vs. 47% in good, p=0.25) between good and poor prognosis groups (Supplemental Table 3) distinguished this signature from established endometrial luteal phase timing phenotypes (displaced or on-time). Therefore, the significant differences (p<0.0001) between the reproductive outcomes of women predicted to have poor and good endometrial prognoses validated the clinical relevance of our transcriptomic signature. Specifically, poor endometrial prognosis was associated with a 34.5% decline in PR (p=3.8E-05), a 52% reduction in LBR (p=5E-10), a 19.6% rise in CMR (p=0.0066), and 20.4% increase in BMR (p=0.0023) (Figure 2A). Further, patients with a poor endometrial prognosis only achieved a CPR of 42.3% after the ninth SET, while patients with a good prognosis had an 83.7% CPR at the fifth attempt (Figure 2B).

The relative risk of implantation failure or miscarriage in women predicted to have poor endometrial prognosis was respectively 2.7 and 11.5 compared to women with good endometrial prognosis. However, when failures in implantation or ongoing pregnancy were considered together, the relative risk of endometrial failure (not achieving a live birth in the next SET) for patients with poor endometrial prognosis was 3.3.

EFR signature biomarker's predictive capability

The 186 samples labelled with poor (n=137) or good (n=49) endometrial prognoses were used to evaluate the signature's predictive performance. The 122 differentially expressed genes between poor/good endometrial prognoses proposed as the EFR biomarker signature were employed to train the model. Cross-validation yielded a median accuracy of 0.92 (min=0.88, max=0.94), sensitivity of 0.96 (min=0.91, max=0.98), and specificity of 0.84 (min=0.77, max=0.88) (Figure 2C). Notably, 163/186 (87.6%) samples were classified correctly in almost 90% of all cross-validation models, while 151/186 (81.2%) samples were well-classified correctly in 100% of the iterations. Twelve and eleven samples were misclassified consistently, in <50% or 50–90% of models, respectively (Figure 2D).

Clinical algorithm results after evaluating both WOI factors.

Next, we grouped samples according to both potential causes of implantation failure, endometrial luteal phase timing (displaced or on-time) and endometrial disruption (good or poor prognosis) and compared the patients' reproductive outcomes. There were no significant differences between the patients with displaced and on-time WOI in terms of BMI (p=0.8740), average number of SETs (p=0.0879), and embryo quality (p=1). However, patients with a displaced WOI were significantly older (40.4 vs. 38.3 years old; p=0.0044) (Supplemental Table 4). Once patients were stratified by prognosis (endometrial disruption), the proportion of patients with poor prognosis was similar (p=0.2458) between displaced and on-time groups.

Experimental validation of genes related to the EFR signature

The expression of the top four differentially expressed genes in the poor prognosis group was validated by RT-qPCR. Progestagen-associated endometrial protein

(*PAEP*) and G-coupled protein receptor 110 (*GPR110*), which were found up-regulated by RNA-seq, were significantly overexpressed in the poor prognosis group, compared to good prognosis group [FC=6.157 (p=0.0288) and FC=11.803 (p=0.0350), respectively; Supplemental Figures 6A-B]. Meanwhile, the expression of fibrinogen beta chain (*FGB*) and solute carrier 16 member 6 (*SLC16A6*), which were found down-regulated by RNA-seq, did not reach a statistically significant difference [FC=1.582 (p=0.2475) and FC=2.311 (p=0.4376), respectively; Supplemental Figures 6C-D].

DISCUSSION

Advances in the diagnosis and treatment of RIF have been limited by its elusive etiology, the discrepancies in clinical classification (mainly due to the lack of consensus over the minimum number of pregnancy attempts) (9,10), and the heterogeneous molecular profiles of affected patients (15). Based on current clinical practice, patients with RIF may be misclassified and/or receive inefficient treatment (9,10). Thus, the aim of this study was to propose a novel gene expression signature that could identify endometrial disruptions independent of endometrial luteal phase timing. Using a semi-supervised learning artificial intelligence strategy together with the endometrial gene expression obtained from our custom EFR panel, we stratified patients according to poor or good endometrial prognoses and demonstrated how this signature reliably predicted gene expression patterns that corresponded with significant differences in PR, LBR, CMR and BMR. When considering both WOI factors (disruption and timing) in our study cohort, poor endometrial prognoses (disruption) affected 73.7% of patients, whereas WOI displacements only affected 54.3%; 41.9% of patients presented a displaced WOI and were predicted to have a

poor endometrial prognosis, while only 12.4% of patients presented with a displaced WOI and were predicted to have a good endometrial prognosis. These results offer a possible explanation as to why other studies reported there was no clinical benefit of personalizing embryo transfers based on transcriptomic dating of the endometrium (34). According to our clinical algorithm, only patients with a displaced WOI and a good endometrial prognosis (12.4% of our cohort) would be better off with this approach. Patients with poor endometrial prognosis (73.7% of our cohort) would have suboptimal reproductive outcomes even though their WOI was on-time. This highlights an unmet healthcare need for IVF patients with endometrial disruptions (18) and underscores the importance of additional prospective studies to further characterize patients based on these two molecular causes for trying tailored treatments.

Contemplating endometrial luteal phase timing together with a prevalent disruption or poor endometrial prognosis shifts the paradigm in studies about the endometrium. Our innovative methodology based on transcriptomics and AI models led us to develop new endometrial biomarker taxonomies related to endometrial luteal phase timing and/or endometrial disruption (16,18). There were 30 genes overlapping between the previously published TED signature (17) and the EFR signature presented herein, emphasizing their correlation despite the lower fold change of biomarkers for endometrial disruption versus endometrial timing (16).

AI algorithms offer powerful approaches for patient stratification, by combining high-throughput molecular data and clinical variables (45). Clinical translation of these approaches will require careful supervision of how the machine learning is initially trained (46). However, semi-supervised learning methodology implementing accurate

clinical diagnostic criteria and patient-specific genomic data to establish relevant molecular taxonomies will be indispensable for advancing precision medicine (23) especially within the context of endometrial-factor infertility. Predictive biomarkers can stratify patients with endometrial failure even if the number of their attempts were insufficient to meet clinical RIF classification criteria (41). To our knowledge, this is the first study to apply semi-supervised learning to the endometrium, conferring an advantage over previous models that were only trained with clinical classifications and did not leverage the underlying molecular heterogeneity of the condition (15). The lack of gene expression differences between RIF and control patients with our initial clinical classification reinforced findings from Macklon´s group and the molecular heterogeneity among RIF patients (15,16).

The EFR signature comprised 122 genes, including 44 genes newly associated to an endometrial gene expression signature and a single common gene with Koot's pioneer endometrial timing-independent signature for endometrial pathology (15). Here, we only considered biopsies collected in the endometrial mid-secretory phase, when patients had received progesterone for 82 to 172 h. Although this signature is independent of endometrial luteal phase timing, further studies are required to confirm if the signature is detectable in other phases of the endometrial cycle. *PAEP* is well characterized in endometrial tissue and was the most up-regulated gene (FC=3.18) in the poor endometrial prognosis profile. However, the levels we observed were 10-fold lower compared to previous studies where changes in endometrial timing were considered (19,47). Alternatively, *FGB,* related to the plasma membrane and vesicle transport by secretory granules, was the most down-regulated gene. This gene accumulated polymorphisms that hinder production of fibrinogen and its associated

anti-inflammatory activity (48) and was recently related to the dysregulated pathways in RIF (49). FOXP1, the most predictive gene, is a transcription factor mediated by estrogen that has established functions in regulation, leukocyte differentiation, and response to lipids and chemokines. This gene is associated to breast (50) and endometrial cancer (51), and endometriosis-related fibrosis (52), but was never included in an endometrial gene signature until now. With *FOXP1* and the FOX transcription factor family being associated with regulation of the menstrual cycle and implantation (53–56), this evidence reinforces our prior study (57) and affirms that alterations in endometrial regulation are an underlying cause of endometrial failure.

Our clinical algorithm considers the two WOI factors, endometrial timing and disruption, to stratify IVF patients based on four possible phenotypes: displaced/on-time and poor/good prognosis. This model is promising for preventive and precision medicine in endometrial-factor infertility, as it combines the robust prediction parameters of the TED model (17) and the EFR biomarker signature's predictive capability reported herein. In contrast to other transcriptomic-based endometrial dating tools (17,19,58–60), our bioinformatic methodology removes the molecular variation associated to the cyclic menstrual changes, providing deeper insights for identifying a new kind of disruption independent of endometrial luteal phase timing by the EFR signature. Further, the EFR biomarker signature was developed based on reproductive outcomes and effectively classifies patients predicted to have positive or negative reproductive outcomes in the first SET following biopsy collection. All these facts, point out to a more potential clinical utility than existing tools that only predict the window of implantation without showing significant differences in reproductive outcomes as have been reported (27–34) and we have shown in our findings. While

our strategy appears promising, the classification presented herein needs further refinement prior to clinical implementation. Larger sample sizes and validation in independent samples are required to ensure model generalization (61). Healthcare professionals will need to be adequately trained to ensure technical reproducibility. Longitudinal assessments including several menstrual cycles in the same patient are recommended to confirm inter-cycle reproducibility and to gain a comprehensive understanding of the reliability of the EFR panel. Additional studies should assess the relationship between a poor endometrial prognosis and the presence of benign disorders that potentially compromise endometrial function and/or embryo implantation (62).

Inspired by the MammaPrint risk signature for breast cancer (63,64), the EFR signature could become a next-generation tool used to classify patients based on endometrial prognosis, to predict reproductive outcomes prior to undergoing IVF, potentially experiencing RIF and/or losing valuable embryos. While treatments for patients with poor endometrial prognosis remain to be determined, clinically identifying these patients is the first step towards improving their care.

AUTHORS' ROLES

Original idea and study design was conceived by P.D.-G. and A.P. Patient population was defined by A.P., M.C.V., I.S.-R. and P.D.-G. Ethical committee was passed by P.D-G with the help of M.C.V. Sample collection and clinical data management were carried out by A.P., N.P., M.C.V., I.S.-R. with the help of J.M.S.-R., D.M.-G, A.M.-M and P.S.-L., supervised by P.D.-G. RNA-seq custom panel was designed by P.D.-G.

and implemented by P.S.-L. and J.M.S.-R. Selection and bioinformatic preprocessing of transcriptomic datasets from GEO were performed by A.D.-P. and P.S.-L. and supervised by P.D.-G. Sample preprocessing and RNA extraction were done by J.M.S.-R. supervised by P.D.-G. Targeted RNA-seq experimental protocol and sequencing was refined and implemented by K.S., coordinated by P.D.-G., and supervised by D.W. Validation design and real-time PCRs were done by D.M.-G and A.M.-M. supervised by P.D.-G. Prediction model design and implementation were done by P.S.-L. and supervised by P.D.-G. Transcriptomic analysis and statistics were analyzed by P.S.-L. with the help of A.D.-P. supervised by P.D.-G. Clinical data analysis was done by P.S.-L. supervised by P.D.-G. Data interpretation and conclusions were provided by P.D.-G., with the help of P.S.-L. and A.D.-P. and supervised by A.P. Tables and figures were designed by P.D.-G. with the help of P.S.-L. and implemented by P.S.-L. Manuscript writing was done by P.D.-G. and P.S.-L., with the help of D.M.-G. supervised by A.P., and revised by all authors.

ACKNOWLEDGEMENTS

The authors thank the patients who participated in the study and the clinical staff who contributed to patient recruitment and organization, especially Laura Caracena, Dr. Marga Esbert, Isabel Llorens, Cristina Gaya, Monica Toribio, and Fernando Quintana. We thank Dr. Ester Castillo (Illumina support, Spain), and Dr. Kira Yanowsky (Genycell Biotech, Spain) for their technical support during RNA-sequencing. We also thank Cristina Cardona (Genomic Analysis Facility of the IIS La Fe) for measuring RNA quality and supporting the first steps of the RNA-sequencing protocol design and library preparation, and Dr. Raquel Amigo (Biobank of the IIS La Fe) for extracting

RNA from endometrial samples. The authors thank Rosalba Lopez for her constructive criticism and editorial services in preparing the manuscript for publication.

Funding

This research was funded by the IVI Foundation (1810-FIVI-066-PD and 1810-FIVI-048-PD). P.D.-G. was supported by the Instituto de Salud Carlos III (ISCIII; Spanish Ministry of Science and Innovation) through the Miguel Servet program (CP20/00118) co-founded by the European Union, and a visiting scientist fellowship funded by the Generalitat Valenciana at Oxford University (BEST/2019/121). P.S.-L. was funded by ISCIII through the Sara Borrell program (CD21/0132) co-founded by the European Union. Financial support to researchers was also provided by the Spanish Ministry of Science, Innovation and Universities (APOTIP/2021/048 [A.D.-P], CIAPOT/2021/13 [A.M.-M], ACIF/2018/072 [J.M.S.-R] and FPU/19/03247 [D.M.-G.]).

Data availability statement

The data underlying this article are available in the article and in its online Supplementary Material.

REFERENCES

1. Noyes RW, Hertig AT, Rock J. Dating the endometrial biopsy. American Journal of Obstetrics and Gynecology 1975;122:262–3.
2. Harper MJK. The implantation window. Baillière's Clinical Obstetrics and Gynaecology 1992;6:351–71.
3. Wilcox AJ, Baird DD, Weinberg CR. Time of Implantation of the Conceptus and Loss of Pregnancy. N Engl J Med 1999;340:1796–9.
4. Murphy CR. Uterine receptivity and the plasma membrane transformation. Cell Res 2004;14:259–67.

5. Talbi S, Hamilton AE, Vo KC, Tulac S, Overgaard MT, Dosiou C, et al. Molecular Phenotyping of Human Endometrium Distinguishes Menstrual Cycle Phases and Underlying Biological Processes in Normo-Ovulatory Women. Endocrinology 2006;147:1097–121.

6. Duc-Goiran P, Mignot TM, Bourgeois C, Ferré F. Embryo–maternal interactions at the implantation site: a delicate equilibrium. European Journal of Obstetrics & Gynecology and Reproductive Biology 1999;83:85–100.

7. Díaz-Gimeno P, Ruiz-Alonso M, Sebastian-Leon P, Pellicer A, Valbuena D, Simón C. Window of implantation transcriptomic stratification reveals different endometrial subsignatures associated with live birth and biochemical pregnancy. Fertility and Sterility 2017;108:703-710.e3.

8. Garrido-Gomez T, Dominguez F, Quiñonero A, Diaz-Gimeno P, Kapidzic M, Gormley M, et al. Defective decidualization during and after severe preeclampsia reveals a possible maternal contribution to the etiology. Proc Natl Acad Sci USA [Internet] 2017 [cited 2024 Jan 10];114. Available from: https://pnas.org/doi/full/10.1073/pnas.1706546114

9. Cimadomo D, Craciunas L, Vermeulen N, Vomstein K, Toth B. Definition, diagnostic and therapeutic options in recurrent implantation failure: an international survey of clinicians and embryologists. Human Reproduction 2021;36:305–17.

10. Pirtea P, Cedars MI, Devine K, Ata B, Franasiak J, Racowsky C, et al. Recurrent implantation failure: reality or a statistical mirage? Fertility and Sterility 2023;120:45–59.

11. Coughlan C, Ledger W, Wang Q, Liu F, Demirol A, Gurgan T, et al. Recurrent implantation failure: definition and management. Reproductive BioMedicine Online 2014;28:14–38.

12. Polanski LT, Baumgarten MN, Quenby S, Brosens J, Campbell BK, Raine-Fenning NJ. What exactly do we mean by 'recurrent implantation failure'? A systematic review and opinion. Reproductive BioMedicine Online 2014;28:409–23.

13. Craciunas L, Gallos I, Chu J, Bourne T, Quenby S, Brosens JJ, et al. Conventional and modern markers of endometrial receptivity: a systematic review and meta-analysis. Human Reproduction Update 2019;25:202–23.

14. Pirtea P, De Ziegler D, Tao X, Sun L, Zhan Y, Ayoubi JM, et al. Rate of true recurrent implantation failure is low: results of three successive frozen euploid single embryo transfers. Fertility and Sterility 2021;115:45–53.

15. Koot YEM, Van Hooff SR, Boomsma CM, Van Leenen D, Koerkamp MJAG, Goddijn M, et al. An endometrial gene expression signature accurately predicts recurrent implantation failure after IVF. Scientific Reports 2016;6:1–12.

16. Devesa-Peiro A, Sebastian-Leon P, Pellicer A, Diaz-Gimeno P. Guidelines for biomarker discovery in endometrium: correcting for menstrual cycle bias reveals new genes associated with uterine disorders. Molecular Human Reproduction 2021;27:gaab011.

17. Diaz-Gimeno P, Sebastian-Leon P, Sanchez-Reyes JM, Spath K, Aleman A, Vidal C, et al. Identifying and optimizing human endometrial gene expression signatures for endometrial dating. Human Reproduction 2022;37:284–96.

18. Sebastian-Leon P, Garrido N, Remohí J, Pellicer A, Diaz-Gimeno P. Asynchronous and pathological windows of implantation: two causes of recurrent implantation failure†. Human Reproduction 2018;33:626–35.

19. Díaz-Gimeno P, Horcajadas JA, Martínez-Conejero JA, Esteban FJ, Alamá P, Pellicer A, et al. A genomic diagnostic tool for human endometrial receptivity based on the transcriptomic signature. Fertility and Sterility 2011;95:50-60.e15.

20. Díaz-Gimeno P, Ruiz-Alonso M, Blesa D, Bosch N, Martínez-Conejero JA, Alamá P, et al. The accuracy and reproducibility of the endometrial receptivity array is superior to histology as a diagnostic method for endometrial receptivity. Fertility and Sterility 2013;99:508–17.

21. Henarejos-Castillo I, Aleman A, Martinez-Montoro B, Gracia-Aznárez FJ, Sebastian-Leon P, Romeu M, et al. Machine Learning-Based Approach Highlights the Use of a Genomic Variant Profile for Precision Medicine in Ovarian Failure. JPM 2021;11:609.

22. Guttmacher AE, Collins FS. Genomic Medicine — A Primer. N Engl J Med 2002;347:1512–20.

23. Mirnezami R, Nicholson J, Darzi A. Preparing for precision medicine. N Engl J Med 2012;366:489–91.

24. Bell J. Stratified medicines: towards better treatment for disease. The Lancet 2014;383:S3–5.

25. Fröhlich H, Balling R, Beerenwinkel N, Kohlbacher O, Kumar S, Lengauer T, et al. From hype to reality: data science enabling personalized medicine. BMC Med 2018;16:150.

26. Krzyszczyk P, Acevedo A, Davidoff EJ, Timmins LM, Marrero-Berrios I, Patel M, et al. The growing role of precision and personalized medicine for cancer treatment. Technology 2018;06:79–100.

27. Cozzolino M, Diáz-Gimeno P, Pellicer A, Garrido N. Use of the endometrial receptivity array to guide personalized embryo transfer after a failed transfer attempt was associated with a lower cumulative and per transfer live birth rate during donor and autologous cycles. Fertility and Sterility 2022;118:724–36.

28. Cozzolino M, Diaz-Gimeno P, Pellicer A, Garrido N. Evaluation of the endometrial receptivity assay and the preimplantation genetic test for aneuploidy in overcoming recurrent implantation failure. J Assist Reprod Genet 2020;37:2989–97.

29. Simón C, Gómez C, Cabanillas S, Vladimirov I, Castillón G, Giles J, et al. A 5-year multicentre randomized controlled trial comparing personalized, frozen and fresh blastocyst transfer in IVF. Reproductive BioMedicine Online 2020;41:402–15.

30. Ben Rafael Z. Endometrial Receptivity Analysis (ERA) test: an unproven technology. Human Reproduction Open 2021;2021:hoab010.

31. Lensen S, Wilkinson J, Van Wely M, Farquhar C. Comments on the methodology of an endometrial receptivity array trial. Reproductive BioMedicine Online 2021;42:283.

32. Bassil R, Casper R, Samara N, Hsieh T-B, Barzilay E, Orvieto R, et al. Does the endometrial receptivity array really provide personalized embryo transfer? J Assist Reprod Genet 2018;35:1301–5.

33. Ruiz-Alonso M, Valbuena D, Gomez C, Cuzzi J, Simon C. Endometrial Receptivity Analysis (ERA): data versus opinions. Human Reproduction Open 2021;2021:hoab011.

34. Doyle N, Jahandideh S, Hill MJ, Widra EA, Levy M, Devine K. Effect of Timing by Endometrial Receptivity Testing vs Standard Timing of Frozen Embryo Transfer on Live Birth in Patients Undergoing In Vitro Fertilization: A Randomized Clinical Trial. JAMA 2022;328:2117.

35. Edgar R. Gene Expression Omnibus: NCBI gene expression and hybridization array data repository. Nucleic Acids Research 2002;30:207–10.

36. Ritchie ME, Phipson B, Wu D, Hu Y, Law CW, Shi W, et al. limma powers differential expression analyses for RNA-sequencing and microarray studies. Nucleic Acids Research 2015;43:e47–e47.

37. Frank E, Hall MA, Witten IH, editors. Data mining: practical machine learning tools and techniques. Fourth Edition. Amsterdam: Elsevier; 2017.

38. Noble WS. What is a support vector machine? Nat Biotechnol 2006;24:1565–7.

39. Breiman L. Random Forests. Machine Learning 2001;45:5–32.

40. Hornik K, Buchta C, Zeileis A. Open-source machine learning: R meets Weka. Comput Stat 2009;24:225–32.

41. Triguero I, García S, Herrera F. Self-labeled techniques for semi-supervised learning: taxonomy, software and empirical study. Knowl Inf Syst 2015;42:245–84.

42. Kanehisa M. KEGG: Kyoto Encyclopedia of Genes and Genomes. Nucleic Acids Research 2000;28:27–30.

43. Ashburner M, Ball CA, Blake JA, Botstein D, Butler H, Cherry JM, et al. Gene Ontology: tool for the unification of biology. Nat Genet 2000;25:25–9.

44. Wickham H. ggplot2: Elegant Graphics for Data Analysis [Internet]. New York, NY: Springer New York; 2009 [cited 2023 Feb 15]. Available from: https://link.springer.com/10.1007/978-0-387-98141-3

45. Zhang W, Yu Y, Hertwig F, Thierry-Mieg J, Zhang W, Thierry-Mieg D, et al. Comparison of RNA-seq and microarray-based models for clinical endpoint prediction. Genome Biol 2015;16:133.

46. Lo Vercio L, Amador K, Bannister JJ, Crites S, Gutierrez A, MacDonald ME, et al. Supervised machine learning tools: a tutorial for clinicians. J Neural Eng 2020;17:062001.

47. Pathare ADS, Zaveri K, Hinduja I. Downregulation of genes related to immune and inflammatory response in IVF implantation failure cases under controlled ovarian stimulation. American J Rep Immunol 2017;78:e12679.

48. Schwedler C, Heymann G, Bukreeva L, Hoppe B. Association of Genetic Polymorphisms of Fibrinogen, Factor XIII A-Subunit and α2-Antiplasmin with Fibrinogen Levels in Pregnant Women. Life 2021;11:1340.

49. Feng X, Meng X, Guo S, Li K, Wang L, Ai J. Identification of key genes and immune cell infiltration in recurrent implantation failure: A study based on integrated analysis of multiple microarray studies. American J Rep Immunol 2022;88:e13607.

50. Ijichi N, Ikeda K, Horie-Inoue K, Inoue S. FOXP1 and Estrogen Signaling in Breast Cancer [Internet]. In: Vitamins & Hormones. Elsevier; 2013 [cited 2024 Jan 10]. p. 203–12.Available from: https://linkinghub.elsevier.com/retrieve/pii/B978012416673800006X

51. Mizunuma M, Yokoyama Y, Futagami M, Horie K, Watanabe J, Mizunuma H. FOXP1 forkhead transcription factor is associated with the pathogenesis of endometrial cancer. Heliyon 2016;2:e00116.

52. Shao X, Wei X. FOXP1 enhances fibrosis via activating Wnt/β-catenin signaling pathway in endometriosis. Am J Transl Res 2018;10:3610–8.

53. Vasquez YM, Wang X, Wetendorf M, Franco HL, Mo Q, Wang T, et al. FOXO1 regulates uterine epithelial integrity and progesterone receptor expression critical for embryo implantation. PLoS Genet 2018;14:e1007787.

54. Ferreira EM, Giorgi VSI, Rodrigues JK, De Andrade AZ, Junior AAJ, Navarro PA. Systemic oxidative stress as a possible mechanism underlying the pathogenesis of mild endometriosis-related infertility. Reproductive BioMedicine Online 2019;39:785–94.

55. Adiguzel D, Celik-Ozenci C. FoxO1 is a cell-specific core transcription factor for endometrial remodeling and homeostasis during menstrual cycle and early pregnancy. Human Reproduction Update 2021;27:570–83.

56. Sebastian-Leon P, Devesa-Peiro A, Aleman A, Parraga-Leo A, Arnau V, Pellicer A, et al. Transcriptional changes through menstrual cycle reveal a global transcriptional derepression underlying the molecular mechanism involved in the window of implantation. Molecular Human Reproduction 2021;27:gaab027.

57. Parraga-Leo A, Sebastian-Leon P, Devesa-Peiro A, Marti-Garcia D, Pellicer N, Remohi J, et al. Deciphering a shared transcriptomic regulation and the relative contribution of each regulator type through endometrial gene expression signatures. Reprod Biol Endocrinol 2023;21:84.

58. Enciso M, Carrascosa JP, Sarasa J, Martínez-Ortiz PA, Munné S, Horcajadas JA, et al. Development of a new comprehensive and reliable endometrial receptivity map (ER Map/ER Grade) based on RT-qPCR gene expression analysis. Human Reproduction 2018;33:220–8.

59. Altmäe S, Koel M, Võsa U, Adler P, Suhorutšenko M, Laisk-Podar T, et al. Meta-signature of human endometrial receptivity: a meta-analysis and validation study of transcriptomic biomarkers. Sci Rep 2017;7:10077.

60. Lipecki J, Mitchell AE, Muter J, Lucas ES, Makwana K, Fishwick K, et al. EndoTime: non-categorical timing estimates for luteal endometrium. Human Reproduction 2022;37:747–61.

61. Ying X. An Overview of Overfitting and its Solutions. J Phys: Conf Ser 2019;1168:022022.

62. Devesa-Peiro A, Sebastian-Leon P, Garcia-Garcia F, Arnau V, Aleman A, Pellicer A, et al. Uterine disorders affecting female fertility: what are the molecular functions altered in endometrium? Fertility and Sterility 2020;113:1261–74.

63. van 't Veer LJ, Dai H, van de Vijver MJ, He YD, Hart AAM, Mao M, et al. Gene expression profiling predicts clinical outcome of breast cancer. Nature 2002;415:530–6.

64. van de Vijver MJ, He YD, van 't Veer LJ, Dai H, Hart AAM, Voskuil DW, et al. A Gene-Expression Signature as a Predictor of Survival in Breast Cancer. N Engl J Med 2002;347:1999–2009.

FIGURE & TABLE LEGENDS

Figure 1. Transcriptomic and functional characterization of the endometrial failure risk (EFR) signature. (A) Volcano plot showing the 122 EFR signature genes. Red and blue dots were used to differentiate EFR genes that were significantly up-regulated or down-regulated in poor prognosis samples, respectively, while grey dots represented genes (n=282) whose expression was not significantly different (FDR>0.05) between poor and good prognoses groups and were not included in EFR signature. **(B)** Principal component analysis highlighting the transcriptomic behaviour of endometrial samples from patients predicted to have poor (orange) or good (green) endometrial prognosis based on genes included in EFR signature. Notably, the transcriptomic variance explained by the first and second principal components (PC1 and PC2, respectively) reached 23.1%. **(C)** Pie chart depicting the overall proportion of EFR signature genes included in each functional category. **(D)** The EFR signature genes were classified into 39 functional groups. Red and blue bars were used to differentiate genes that were significantly up-regulated or down-regulated in poor prognosis samples, respectively. Figure created with BioRender.com.

Figure 2. Clinical meaning and prediction capability of the EFR signature. (A) Clinical outcomes of the single embryo transfer following biopsy collection. Rates for pregnancy, live birth, clinical and biochemical miscarriage were calculated as described in the Supplemental Methods. Statistical differences were evaluated using Fisher's exact test. **(B)** Comparison of cumulative pregnancy rates. Notably, many patients predicted to have a good endometrial prognosis achieved pregnancy with a single transfer (63.3%) and reached the maximum number of pregnancies (83.7%) at the fifth transfer, while patients predicted to have poor endometrial prognosis were only able to achieve a cumulative pregnancy rate of 42.3% at the ninth transfer. **(C)** Boxplots for the EFR signature prediction parameters (sensitivity, specificity, and accuracy) calculated over 100 iterations of 5-fold stratified cross-validation. **(D)** Histogram showing the proportion of patients that were successfully classified during the aforementioned cross-validation procedure. Figure created with BioRender.com.

Figure 3. Evaluation of reproductive outcomes following single embryo transfer (SET) based on the two WOI factors. Patients were initially classified according to transcriptomic endometrial dating by TED (28) **(A)**, as per current clinical practice. This approach distinguishes between patients whose window of implantation (WOI) was considered displaced or on time. These groups were then stratified according to their endometrial disruption **(B)**, as determined by our semi-supervised stratification. In all cases, the reproductive outcomes of the first SET after biopsy collection were compared using Fisher´s exact test. (NS) = No significant differences; *p<0.05; **p<0.01; ***p<0.001. Figure created with BioRender.com.

Table 1. Endometrial Failure Risk (EFR) Signature´s genes. Complete list of the 122 genes included in the endometrial failure risk (EFR) signature. Gene name and ID, Fold change (FC) related to poor prognosis and adjusted p-value by false discovery rate (FDR) are indicated.

Supplemental Figure 1. Study design. (1) The 404-gene Endometrial Failure Risk (EFR) panel comprising genes related to endometrial dating and/or recurrent implantation failure (RIF) was employed for custom RNA-sequencing in 217 patients that met quality criteria. The transcriptomic profiles obtained with the EFR panel were corrected for the effect endometrial luteal phase timing using the TED model. **(2)** Patients were broadly classified according to an acute clinical classification (aRIF or aFertile) based on how many IVF attempts it took to achieve a full-term pregnancy and a semi-supervised learning procedure was then used to predict whether these patients had a poor or good endometrial prognosis based on their transcriptomic profile. Reproductive outcomes were compared between the two prognosis groups. **(3)** Differentially expressed genes between the prognosis groups were established as the EFR biomarker signature. **(4)** The prognostic EFR signature was cross-validated (5-fold, 100 times) to evaluate the predictive performance and capability to reliably distinguish between prognosis groups. Figure created with BioRender.com.

Supplemental Figure 2. In silico gene selection procedure for Endometrial Failure Risk (EFR) panel. The EFR panel was compiled from two different sources. The GSE58144 whole-transcriptome dataset from GEO was preprocessed according to the artificial intelligence (AI)-based taxonomy described in Sebastian-Leon et al., 2018. Endometrial progression was corrected following guidelines for biomarker discovery in the endometrium (16). This data was them employed for an in silico pathological gene discovery (28). Then, a transcriptomic endometrial dating (TED) signature (28) was added to the EFR panel to correct for endometrial displacement bias. Figure created with BioRender.com.

Supplemental Figure 3. Endometrial Failure Risk (EFR) dataset preprocessing. (A) Number of sequencing reads per sample. Colors indicate the nine different sequencing runs. Samples with fewer than 2 million reads were considered low-quality samples and were excluded from subsequent analysis (n=6, indicated with vertical black arrows). **(B)** Distribution of Voom and quantiles-normalized expression data pointed two samples with anomalous

behavior (indicated with black vertical arrows) that were excluded from further analysis. Principal components analyses highlighted batch effects related to the **(C)** sequencing run and (D) endometrial displacement classified by TED model. Linear models were used to correct each effect. PC1: First principal component. PC2: Second principal component. Figure created with BioRender.com.

Supplemental Figure 4. Evaluation of possible batch effects related to clinical and experimental variables. Principal components analysis (PCA) plots for endometrial transcriptomic data. Data were color coded according to: **(A)** patient age (years) at the time of biopsy collection; **(B)** body mass index (BMI) at the time of biopsy [where normal indicates a BMI of <25 kg/m^2, overweight indicates a BMI of 25-30 kg/m^2, and obese indicates a BMI of >30 kg/m^2]; **(C)** the clinic where the biopsy was collected; **(D)** RNA extraction batch; **(E)** RNA integrity number (RIN); **(F)** Percentage of RNA fragments >200 nucleotides (DV200). PC1: First principal component. PC2: Second principal component. Figure created with BioRender.com.

Supplemental Figure 5. Patient stratification process for good and poor prognosis. (A) Initial acute clinical classification of patients was based on the number of single embryo transfers the patients underwent in total n, and whether or not they achieved a full-term pregnancy. In total, 44 patients were classified as acute RIF (aRIF; orange) because they did not achieve full-term pregnancy following ≥3 attempts; 40 patients were classified as acute fertile (aFertile; green) because they achieved a full-term pregnancy at the first attempt; and 133 patients (61%) remained unclassified (grey) for falling between these criteria. **(B)** Our semi-supervised artificial intelligence approach integrating clinical variables and endometrial transcriptomic data redistributed patients (shown by the dotted arrows) into poor (n=137; orange) or good (n=49; green) endometrial prognosis groups, leaving only 14% of patients unclassified (grey). Figure created with BioRender.com.

Supplemental Figure 6. RT-qPCR validation. The top four differentially expressed genes between patients predicted to have poor and good endometrial prognosis were selected for RT-qPCR validation. Bar plots show the relative mRNA expression of (A) PAEP, (B) GPR110, (C) SLC16A6, and (D) FGB in poor (n=10) and good (n=10) prognosis groups. *p<0.05.

Supplemental Figure 7. Variability due to endometrial dating effect correction. In a first step, the endometrial timing effect was constrained by taking biopsies only in mid-secretory phase. In a second step, the remaining endometrial variability was identified by classifying them into four secretory-phases profiles and was corrected for the WOI displacement effect.

Supplemental Table 1. Specific primers used for RT-qPCR. The sequence of the four primer pairs used to determine endometrial PAEP, GPR110, FGB and SLC16A6 gene expression by qRT-PCR are shown. qRT-PCR: quantitative real-time polymerase chain reaction.

Supplemental Table 2: Functional characterization of the 122-gene EFR signature associated with poor endometrial prognosis. Term name is the functional name assigned in Gene Ontology or KEGG databases. *Functional groups were manually grouped under 39 umbrella functions, numbered as follows: Inmune system & inflamation = 1; Regulation = 2; Cell cycle, proliferation & differenciation = 3; Apoptosis = 4; Binding = 5; Adhesion = 6; Metabolism = 7; Nucleic Acids processes = 8; Lipid metabolism & signaling = 9; Proteins processes = 10; Steroidogenesis & Steroid signaling = 11; Nervous system = 12; Cellular membrane = 13; Golgi & ER = 14; Organelles & Vesicles = 15; Catalytic activity = 16; Extracellular matrix = 17; Necroptosis = 18; Signaling = 19; Transport (secretion, endo/exocytosis) = 20; Hormones = 21; Cell migration = 22; Oxidoreductase = 23; Development, growth & morphogenesis = 24; Cytoskeleton & microtubules = 25; Epigenetics

& Gene expression = 26; Glucose homeostasis = 27; Protein degradation = 28; Cell projections & cillia = 29; Muscle contraction/relaxation = 30; Vitamins = 31; Cell senescence & longevity = 32; Ion exchange & homeostasis = 33; Gametogenesis & reproduction = 34; Oxidative stress & response to O2 = 35; Cell action potential & polarization = 36; Cardiovascular, coagulation & blood pressure = 37; Phosphorylation = 38; Other = 0.

Supplemental Table 3. Patient demographics and baseline reproductive characteristics. Continuous variables are presented as mean (standard deviation) and discrete variables were presented as the number of patients and proportion of the total (%). BMI = body mass index; SET = single embryo transfer; Displaced = Out-of-phase endometrium; On time= In-phase endometrium. HEQ = High embryo quality; UEQ = Uncertain embryo quality. ***p<0.001. Endometrial dating according to TED model (See Supplemental Methods).

Supplemental Table 4. Patient demographics, baseline reproductive characteristics and endometrial prognosis by endometrial dating. Continuous variables were presented as mean (standard deviation) and discrete variables were represented as the number of patients and proportion of the total. BMI = body mass index; Displaced= out-of-phase endometrium; On time= in-phase endometrium; SET = single embryo transfer; HEQ = High embryo quality; UEQ = Uncertain embryo quality. **p<0.01; ***p<0.001. Endometrial dating according to TED model (See Supplemental Methods).

Table 1. Endometrial Failure Risk (EFR) Signature´s genes. Complete list of the 122 genes included in the endometrial failure risk (EFR) signature. Gene name and ID, Fold change (FC) related to poor prognosis and adjusted p-value by false discovery rate (FDR) are indicated.

Gene ID	Gene Name	FC	FDR
PAEP	Progestagen Associated Endometrial Protein	3.1873	9.12E-07
GPR110	Adhesion G Protein-Coupled Receptor F1	2.3304	3.68E-05
CHST1	Carbohydrate Sulfotransferase 1	2.0292	0.0004
POSTN	Periostin	1.8936	0.0009
BCL2L10	BCL2 Like 10	1.8549	0.0001
TSPAN8	Tetraspanin 8	1.8098	0.0179
CYP3A5	Cytochrome P450 Family 3 Subfamily A Member 5	1.7966	0.0092
SFRP4	Secreted Frizzled Related Protein 4	1.7778	1.23E-06
BAI2	Adhesion G Protein-Coupled Receptor B2	1.7138	0.0018
ITGA8	Integrin Subunit Alpha 8	1.7033	0.0005
PMEPA1	Prostate Transmembrane Protein, Androgen Induced 1	1.7026	3.35E-07
CLU	Clusterin	1.6771	3.68E-05
MUC16	Mucin 16, Cell Surface Associated	1.6288	0.0001
MYH7B	Myosin Heavy Chain 7B	1.6034	0.0116
SCGB2A2	Secretoglobin Family 2A Member 2	1.5859	0.0326
STC1	Stannioclacin 1	1.5800	0.0033
FOXP1	Forkhead Box P1	1.5332	3.94E-13
C10orf10	DEPP1 Autophagy Regulator	1.5093	0.0004
LRRC17	Leucine Rich Repeat Containing 17	1.5020	0.0001
SERTAD4	SERTA Domain Containing 4	1.4805	7.63E-07
COL16A1	Collagen Type XVI Alpha 1 Chain	1.4786	0.0024
C1orf133	SERTAD4 Antisense RNA 1	1.4381	0.0065
MAPK8IP3	Mitogen-Activated Protein Kinase 8 Interacting Protein 3	1.4275	0.0003
ABCC3	ATP Binding Cassette Subfamily C Member 3	1.4181	0.0124
MFAP5	Microfibril Associated Protein 5	1.4030	0.0033
MFAP2	Microfibril Associated Protein 2	1.3990	0.0005
GPX3	Glutathione Peroxidase 3	1.3960	0.0198
EDN3	Endothelin 3	1.3627	0.0053
SORCS1	Sortilin Related VPS10 Domain Containing Receptor 1	1.3563	0.0322
DUSP2	Dual Specificity Phosphatase 2	1.3545	0.0264

SLPI	Secretory Leukocyte Peptidase Inhibitor	1.3463	0.0197
BICD1	BICD Cargo Adaptor 1	1.3427	1.99E-05
CRABP2	Cellular Retinoic Acid Binding Protein 2	1.3395	0.0040
ARID5B	AT-Rich Interaction Domain 5B	1.3247	1.31E-05
EVC	EvC Ciliary Complex Subunit 1	1.3157	0.0011
C2CD4B	C2 Calcium Dependent Domain Containing 4B	1.3091	0.0109
ANO1	Anoctamin 1	1.3014	0.0053
CLDN4	Claudin 4	1.2867	0.0216
IGF2	Insulin Like Growth Factor 2	1.2854	0.0134
SYNE2	Spectrin Repeat Containing Nuclear Envelope Protein 2	1.2756	5.71E-06
VAV3	Vav Guanine Nucleotide Exchange Factor 3	1.2644	0.0286
ITGA9	Integrin Subunit Alpha 9	1.2562	0.0084
OBFC2A	Nucleic Acid Binding Protein 1	1.2266	0.0032
WEE1	WEE1 G2 Checkpoint Kinase	1.2190	6.54E-06
RAB40B	RAB40B, Member RAS Oncogene Family	1.2100	0.0042
BCL6	BCL6 Transcription Repressor	1.1891	0.0084
ID4	Inhibitor Of DNA Binding 4, HLH Protein	1.1878	0.0156
CD55	CD55 Molecule (Cromer Blood Group)	1.1806	0.0493
LETM2	Leucine Zipper And EF-Hand Containing Transmembrane Protein 2	1.1754	0.0179
CYBRD1	Cytochrome B Reductase 1	1.1647	0.0116
LIMK2	LIM Domain Kinase 2	1.1614	0.0022
C14orf45	Basal Body Orientation Factor 1	1.1526	0.0053
C16orf70	Phagosome Assembly Factor 1	1.1514	0.0022
FOSL2	FOS Like 2, AP-1 Transcription Factor Subunit	1.1412	0.0193
SCAMP1	Secretory Carrier Membrane Protein 1	1.1296	0.0264
CTDSP2	CTD Small Phosphatase 2	1.1099	0.0166
RNF19A	Ring Finger Protein 19A, RBR E3 Ubiquitin Protein Ligase	1.1058	0.0250
HMGN3	High Mobility Group Nucleosomal Binding Domain 3	1.0988	0.0286
ACTN1	Actinin Alpha 1	1.0983	0.0322
ENY2	ENY2 Transcription And Export Complex 2 Subunit	-1.0932	0.0466
PSMB10	Proteasome 20S Subunit Beta 10	-1.1231	0.0053
ARHGDIA	Rho GDP Dissociation Inhibitor Alpha	-1.1245	0.0433
PRPF4	Pre-MRNA Processing Factor 4	-1.1397	0.0348

COPG1	COPI Coat Complex Subunit Gamma 1	-1.1433	0.0006
RACGAP1	Rac GTPase Activating Protein 1	-1.1496	0.0042
PNP	Purine Nucleoside Phosphorylase	-1.1519	0.0143
STEAP4	STEAP4 Metalloreductase	-1.1550	0.0270
BDH1	3-Hydroxybutyrate Dehydrogenase 1	-1.1744	0.0030
ECI2	Enoyl-CoA Delta Isomerase 2	-1.1862	0.0178
ANK3	Ankyrin 3	-1.2084	0.0433
IL15	Interleukin 15	-1.2233	0.0198
GSN	Gelsolin	-1.2241	0.0076
GLIPR1	GLI Pathogenesis Related 1	-1.2251	0.0166
CBR3	Carbonyl Reductase 3	-1.2252	0.0124
ATP6V0E2	ATPase H+ Transporting V0 Subunit E2	-1.2304	0.0082
DYNLT3	Dynein Light Chain Tctex-Type 3	-1.2323	0.0199
S100A4	S100 Calcium Binding Protein A4	-1.2478	0.0041
BUB1B	BUB1 Mitotic Checkpoint Serine/Threonine Kinase B	-1.2482	0.0451
IDH1	Isocitrate Dehydrogenase (NADP(+)) 1	-1.2488	0.0124
PLA2G16	Phospholipase A And Acyltransferase 3	-1.2498	0.0124
EPHB3	EPH Receptor B3	-1.2530	0.0396
OAZ3	Ornithine Decarboxylase Antizyme 3	-1.2581	0.0013
PYCR1	Pyrroline-5-Carboxylate Reductase 1	-1.2597	0.0007
FAM155B	NALCN Channel Auxiliary Factor 2	-1.2618	0.0116
ECHS1	Enoyl-CoA Hydratase, Short Chain 1	-1.2621	3.68E-05
CSRP2	Cysteine And Glycine Rich Protein 2	-1.2647	0.0023
TLR4	Toll Like Receptor 4	-1.2716	0.0065
CTSW	Cathepsin W	-1.2764	0.0322
CEP55	Centrosomal Protein 55	-1.3021	0.0264
BARD1	BRCA1 Associated RING Domain 1	-1.3064	0.0014
PLA2G4A	Phospholipase A2 Group IVA	-1.3101	0.0008
ATP1B1	ATPase Na+/K+ Transporting Subunit Beta 1	-1.3202	0.0113
FOXO1	Forkhead Box O1	-1.3330	0.0018
BIRC3	Baculoviral IAP Repeat Containing 3	-1.3496	0.0007
CRISP3	Cysteine Rich Secretory Protein 3	-1.3498	0.0397
LMCD1	LIM And Cysteine Rich Domains 1	-1.3627	0.0012
PSMB8	Proteasome 20S Subunit Beta 8	-1.3783	3.68E-05
CD81	CD81 Molecule	-1.3888	0.0104

ALDH1A3	Aldehyde Dehydrogenase 1 Family Member A3	-1.3891	0.0007
SQLE	Squalene Epoxidase	-1.3905	0.0001
KMO	Kynurenine 3-Monooxygenase	-1.4107	0.0434
RPRM	Reprimo, TP53 Dependent G2 Arrest Mediator Homolog	-1.4121	0.0061
SPP1	Secreted Phosphoprotein 1	-1.4130	0.0242
ANGPTL1	Angiopoietin Like 1	-1.4381	0.0017
HPRT1	Hypoxanthine Phosphoribosyltransferase 1	-1.4394	1.43E-05
ATP6V1A	ATPase H+ Transporting V1 Subunit A	-1.4484	0.0040
CDK1	Cyclin Dependent Kinase 1	-1.4651	0.0084
ENPEP	Glutamyl Aminopeptidase	-1.4704	0.0441
TH	Tyrosine Hydroxylase	-1.5149	0.0113
G0S2	G0/G1 Switch 2	-1.5183	0.0226
PROS1	Protein S	-1.5297	0.0025
STAR	Steroidogenic Acute Regulatory Protein	-1.5342	0.0005
DKK1	Dickkopf WNT Signaling Pathway Inhibitor 1	-1.5425	0.0005
BANK1	B Cell Scaffold Protein With Ankyrin Repeats 1	-1.5553	0.0005
KCNJ2	Potassium Inwardly Rectifying Channel Subfamily J Member 2	-1.6602	0.0119
SLC7A2	Solute Carrier Family 7 Member 2	-1.6919	0.0038
PROK1	Prokineticin 1	-1.7218	0.0106
OLFM4	Olfactomedin 4	-1.7759	0.0458
IFNG	Interferon Gamma	-1.9666	0.0033
CXCL13	C-X-C Motif Chemokine Ligand 13	-2.0690	0.0001
SLC16A6	Solute Carrier Family 16 Member 6	-2.2113	9.12E-07
FGB	Fibrinogen Beta Chain	-2.3652	0.0108

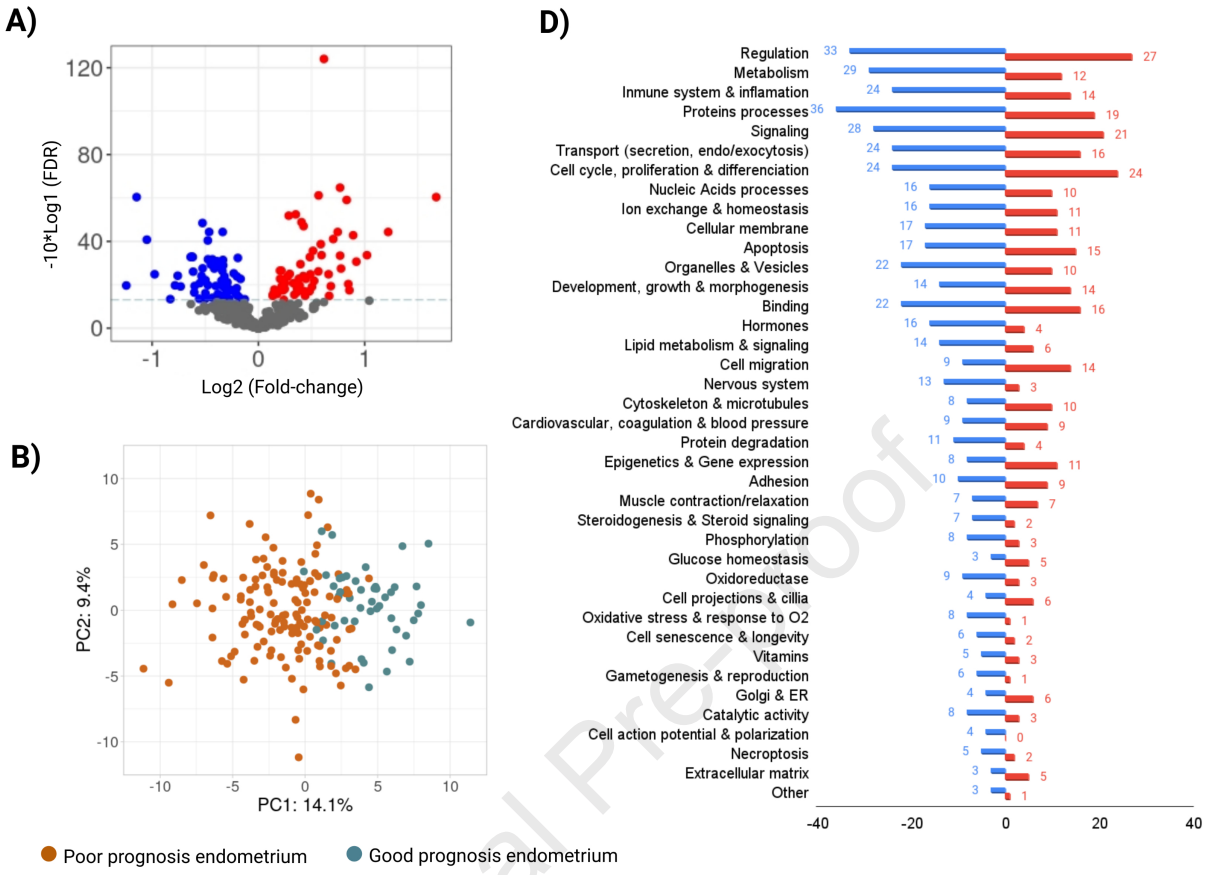

A)

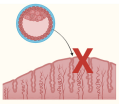

	Poor prognosis 137 (63.1%)	Good prognosis 49 (22.6%)	
Pregnancy rate	44.6%	79.6%	(***)
Live birth rate	25.6%	77.6%	(***)
Clinical miscarriage rate	22.2%	2.6%	(***)
Biochemical miscarriage rate	20.4%	0.0%	(***)

B)

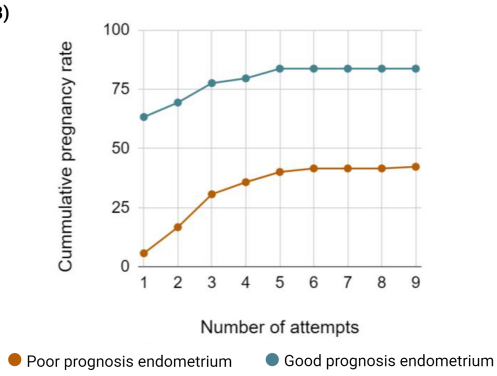

C)

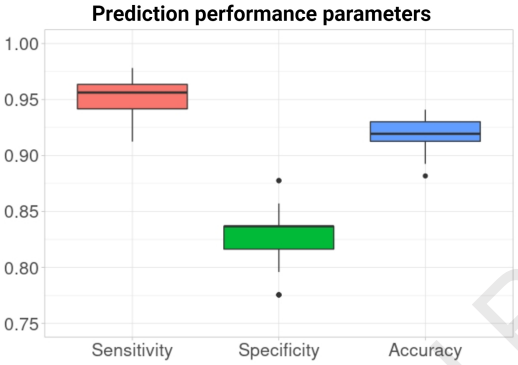

D)

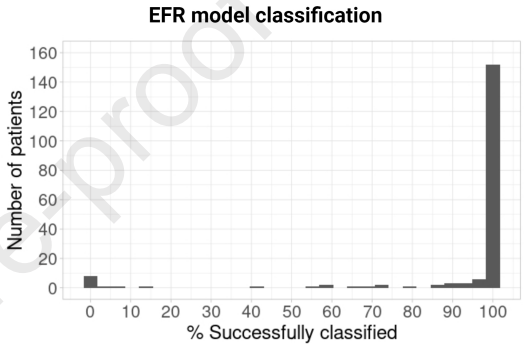

A)

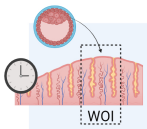

	Displaced WOI 101 (54.3%)	On time WOI 85 (45.7%)	
Pregnancy rate	48.7%	61.8%	(NS)
Live birth rate	34.2%	48.3%	(NS)
Clinical miscarriage rate	13.0%	10.9%	(NS)
Biochemical miscarriage rate	16.7%	10.9%	(NS)

B)

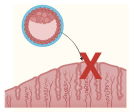

Poor prognosis 78 (77.2%)

Good prognosis 23 (22.8%)

Poor prognosis 59 (69.4%)

Good prognosis 26 (30.6%)